Materials Chemistry and Physics 116 (2009) 119–124

Contents lists available at ScienceDirect

Materials Chemistry and Physics

journal homepage: www.elsevier.com/locate/matchemphys

Aging kinetics of 17-4 PH stainless steel

H. Mirzadeh*, A. Najafizadeh

Department of Materials Engineering, Isfahan University of Technology, Isfahan 84156-83111, Iran

ARTICLE INFO

Article history:
Received 12 October 2008
Received in revised form 6 February 2009
Accepted 22 February 2009

Keywords:
Precipitation hardening
Neural network modeling
Ageing kinetics
Hardness based model

ABSTRACT

The influence of aging condition and the precipitation kinetics of 17-4 PH stainless steel (AISI 630) were studied in this paper. The effect of aging temperature and time in terms of tempering parameter on the strengthening behavior of this steel was modeled and analyzed by means of artificial neural networks (ANNs). The hardening, overaging and softening behaviors in accordance to aging reactions (precipitation and coarsening of Cu, recovery, and reversion of martensite to austenite) were determined from this ANN model. Moreover, Johnson–Mehl–Avrami–Kolmogorov (JMAK) analysis were applied to characterize precipitation kinetics of this martensitic age hardenable alloy. Time exponents (0.465 on average) were within the range reported for maraging steels. The activation energy for precipitation reaction was determined as 262 kJmol^{-1} which is consistent with the activation energy for diffusion of copper in ferrite. Furthermore, precipitation rate showed exponential dependence on aging temperature.

1. Introduction

Among the precipitation hardening stainless steels, martensitic alloys such as 17-4 PH, 15-5 PH and PH 13-8 Mo have special importance due to their very high strength and hardness. 17-4 PH (AISI 630) is more common than any other type of precipitation hardened stainless steels. Its ability to develop very high strength without the catastrophic loss of ductility and its superior corrosion resistance to other steels of similar strength, have made it very attractive to designers and engineers [1–6].

This steel is strengthened by precipitation of copper rich phases in the martensitic matrix through a simple solution treatment and aging practice. The aged condition is generally indicated by the letter "H" followed by the temperature in degrees Fahrenheit at which the aging took place. 17-4 PH stainless steel can be heat treated at a variety of temperatures to develop a wide range of properties. Standard one-step aging treatments applicable to alloy 17-4 PH after the solution treatment are shown in Table 1.

Alloy 17-4 PH exhibits useful mechanical properties in solution-treated condition (called as Condition A) which has been used successfully in numerous applications. The hardness and tensile properties fall within the range of those for Conditions H1100 and H1150. However, in critical applications, the alloy is used in the aged condition, rather than Condition A. Heat treating to the over-aged condition, especially at the higher end of the temperature range (see Table 1), stress-relieves the structure by tempering the martensitic structure and may provide greater toughness and more reliable resistance to stress corrosion cracking (SCC) than in Condition A.

During aging treatment, recovery and reversion of martensite to austenite may occur in addition to the formation and growth of copper precipitates [3–11]. Since the chromium in this alloy is within the spinodal line, phase decomposition of martensite into the Fe-rich α and the Cr-enriched α' is expected during long-term aging (of the order of thousand hours) below 450 °C [7,8].

Since the strength, hardness, toughness and corrosion resistance of 17-4 PH stainless steels vary with aging condition, it is very important to understand the aging response of this alloy. In this paper, the effect of aging temperature and time on the hardening behavior of 17-4 PH stainless steel was modeled and analyzed by means of artificial neural networks (ANNs). ANN is a powerful tool for modeling, especially when the underlying data relationships between the inputs and outputs are unknown. ANN modeling can overcome some of the difficulties associated with other methods. For example, it does not need to choose a (physical) relationship between the parameters before analysis.

2. Methodology

2.1. Database

A relatively large database was taken from the literature [1,3,5,6,9–14]. These data were divided into three groups, 70% for the training set, 15% for the validation set and 15% for the test set. In this paper, the validation set is used to control training process and the testing set is used to evaluate the generalization ability of the trained network. The tempering temperature and time in terms of tempering parameter values are used as input data and the relative

* Corresponding author.
E-mail address: h-m@gmx.com (H. Mirzadeh).

0254-0584/$ – see front matter © 2009 Elsevier B.V. All rights reserved.
doi:10.1016/j.matchemphys.2009.02.049

Table 1
Standard one-step aging treatments for alloy 17-4 PH.

Condition	Temperature (°C)	Aging time (hours)	Cooling
H900	482	1	Air
H925	496	4	Air
H1025	551	4	Air
H1075	580	4	Air
H1100	593	4	Air
H1150	621	4	Air

percentage of hardening values are considered as output data. These parameters will be introduced in the following sections.

2.2. Tempering parameter

Tempering charts usually give hardness as a function of temperature for only one tempering time. However, in practice, tempering times vary frequently, and a method of converting tempering curves for one time to curves for another time would be very valuable. These two variables could be combined in the form of time-compensated temperature which is known as Larson–Miller or Hollomon–Jaffe tempering parameter (P) [15,16] by the equation below:

$$P = T(C + \log t) \times 10^{-3} \quad (1)$$

where T is the absolute temperature in Kelvin and t is the tempering time in hour, while C is the materials constant in the range of 10 to 20, which in many applications considered to be 20.

2.3. Relative percentage of hardening

The as reported hardness values prior to and after aging treatment in different references depend considerably on variations in chemical composition and also hardness measurement technique. In order to overcome this problem, a dimensionless parameter named as *relative percentage of hardening* (H_t) was defined in this study by the equation below:

$$H_t = \left(\frac{H - H_{st}}{H_{st}}\right) \times 100 \quad (2)$$

where, H and H_{st} are the measured hardness of aged and solution-treated specimens, respectively.

2.4. ANN approach

(1) A standard feed-forward network with one hidden layer [17] was used in the present work. Complexity of the model is related to the number of hidden units. An overcomplex network accurately models the training data but generalizes badly [18]. The number of hidden units was determined by the try and error procedure [19–21].
(2) The nonlinear hyperbolic tangent activation function (Eq. (3)) [19] and linear transfer function were used in the hidden and output layers, respectively.

$$y = \tan sig\,(x) = \frac{e^x - e^{-x}}{e^x + e^{-x}} \quad (3)$$

(3) The well-known back-propagation method is usually used to train ANNs. The early standard algorithm usually requires many iterations to converge if it converges at all. Therefore, a number of variations of the standard algorithm have been developed. Among them, the Levenberg–Marquardt is the most popular one [19–21]. This training algorithm was used in this work.
(4) The neural network can be easily overtrained, in which the error rate on new unseen data becomes much larger than the error rate on the training data. Therefore, it is important not to overtrain the network. A good method for choosing the number of training epochs (iterations) is the early stopping technique. In this technique, the training process must be stopped when the error measured using an independent validation set starts to increase [22]. This method was used in the present work.
(5) If the network is properly trained, it has then learned to model the function that relates the input variables to the output variables and can subsequently be used to make predictions where the output is not known. This ability is called generalization [19–21]. In this paper the test set was used to evaluate the generalization ability of the trained network.

The emphasis of this paper is on the applications of ANN as a powerful modeling technique. Therefore, the method used was briefly explained here and more details can be found elsewhere [19–21].

3. Results and discussion

3.1. The aging response

Fig. 1 shows the effect of tempering parameter on the hardening behavior of the solution-treated specimen from data reported in the literature [1,3,5,6,9–14]. The available data is noisy, especially at peak and overaging zones. Therefore, the conventional linear and nonlinear regression methods are inappropriate to model this behavior. Besides that, a common application of artificial intelligence is pattern recognition for the purpose of drawing conclusions based on data [23].

The results of the best nonlinear fitting and obtained curve by ANN method are shown in Fig. 2. The ANN curve has better fit to available data, especially at low and high values of tempering parameter, showing the appropriateness of ANN statistical approach. The ANN curve for relative percentage of hardening and also its derivative (rate of hardening) versus tempering parameter are shown in Fig. 3. The derivative curve was obtained using the central difference approach by the following equation:

$$\left.\frac{dH_t}{dP}\right|_i = \frac{H_t|_{i+1} - H_t|_{i-1}}{P_{i+1} - P_{i-1}} \quad (4)$$

As can be seen in Fig. 3, by increasing tempering parameter, the relative percentage of hardening shows four successive stages:

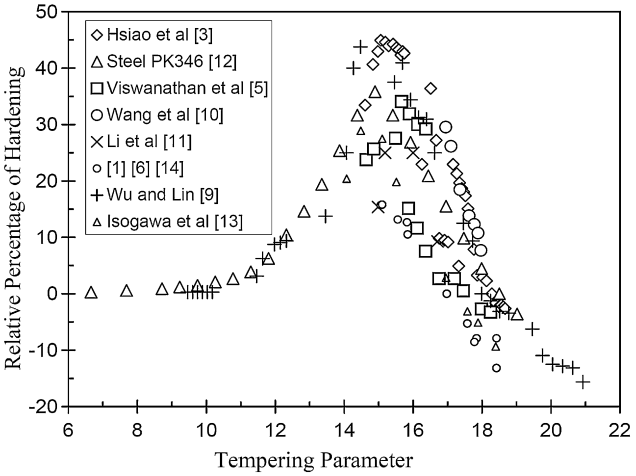

Fig. 1. Effect of tempering parameter on the aging behavior.

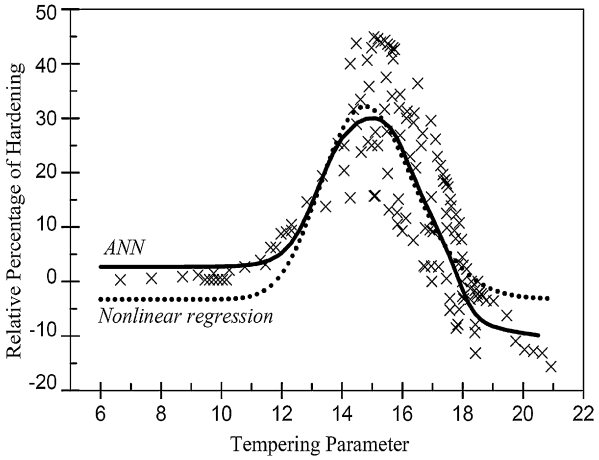

Fig. 2. Nonlinear and ANN curves fitted to available data.

(i) At low tempering parameters up to 10, there is no tangible increase in the relative percentage of hardening. This trend is better understood from the curve of hardening rate (dH_t/dP). This behavior is ascribed to insufficient temperature and time for precipitation of copper phase.

(ii) At the tempering parameters ranging from 10 to 15, the precipitation of copper becomes dominant that leads to increase in hardness. Moreover, the derivative curve shows a peak point at tempering parameter of 13.25 that coincides with an inflection point in hardening curve. This may be attributed to a softening mechanism such as recovery of martensite that becomes more effective at this stage.

(iii) After the peak point of hardening curve up to tempering parameter of 17.9, the relative percentage of hardening continuously decreases. This phenomenon can be attributed to the simultaneous effect of recovery, coarsening of copper precipitates and probably reversion of martensite to austenite. Furthermore, the derivative curve shows that the rate of softening increases by increasing the tempering parameter and finally reaches to a constant value at this range.

(iv) After the tempering parameter of 17.9, the relative percentage of hardening becomes negative. The derivative curve shows that the rate of softening reduces and finally tends to zero value. In this stage, martensite has already been tempered, precipitates have been coarsened and considerable amount of reverted austenite has been formed. Therefore, the impact of aging on hardness will be diminished.

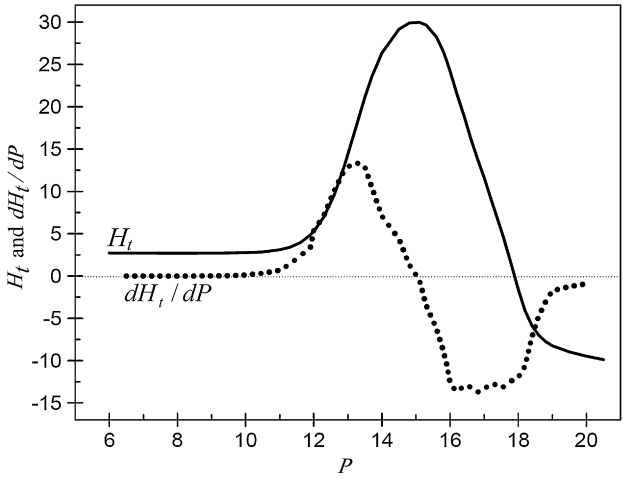

Fig. 3. Relative percentage of hardening (H_t) and its derivative versus tempering parameter (P).

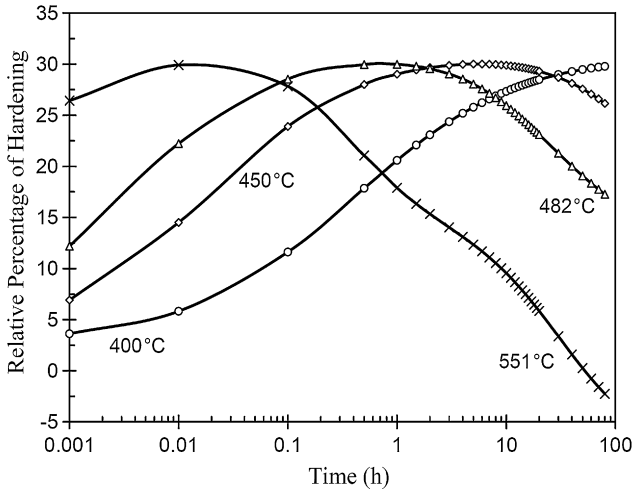

Fig. 4. Effect of aging time on the hardening behavior at various temperatures for 17-4 PH stainless steel.

The maximum hardness is obtained at tempering parameters ranging from 14.5 to 15.5 (e.g. H900 condition) which is suitable for applications requiring high strength and hardness. Aging at tempering parameters ranging from 15.5 to 17.9 (e.g. H1025 condition) generally falls in the overaging condition that is considered for better toughness and greater resistance to stress corrosion cracking. Tempering parameters above 17.9 (e.g. H1150 condition) produce a material softer than the one in the solution-treated condition. The material in this condition is suitable for cold working [6]. It is noteworthy that this steel in the solution-treated condition, which is equivalent to as annealed state of conventional materials, is quite hard.

3.2. Effect of aging time and temperature

Fig. 4 shows the effect of tempering time on the hardening behavior at various aging temperatures. The common characteristics of hardening curves are: (i) the hardness increases gradually at lower temperatures but rapidly at higher temperatures to a peak value, (ii) The time required to achieve peak hardness decreases with increasing temperature and (iii) the hardness decrease beyond peak hardness is more prominent at the higher temperatures. These behaviors are in general agreement with previous investigations [3,24].

Fig. 5 shows the effect of tempering temperature on the hardening behavior at various tempering times. The dependence of hardness on tempering time decreases by increasing temperature up to about 460 °C. After this temperature, the dependence of hardness on tempering time increases again. The highest values of hardness (and also strength) for 17-4 PH stainless steel are generally obtained after aging from 440 to 490 °C (Fig. 5). On the other hand, aging above 595 °C (corresponding to 4 h aging) generally results in material softer than that in the annealed condition. The later phenomenon can be attributed to (i) coarsening of copper precipitates, (ii) recovery and (iii) formation of reverted austenite [3–5,9].

3.3. Avrami analysis

In order to apply the hardness measurements to kinetics analysis, a relationship between the relative percentage of hardening and fraction transformed is required. In typical investigations of this kind, the fraction transformed has been assumed to be linearly

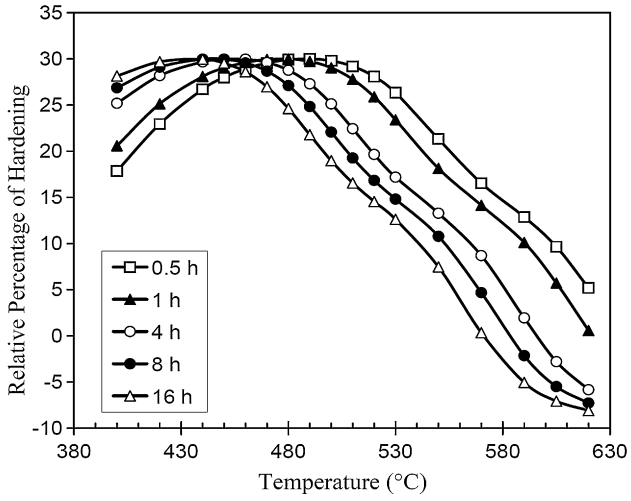

Fig. 5. Effect of temperature on the hardening behavior at various aging times for 17-4 PH stainless steel.

proportional to the change in hardness, resistivity or conductivity values [25–28]. However, a more complex approach (a modification of method described in Reference [24]) is used in this paper. The strength increase ($\Delta\tau$) and also hardness increase (owing to proportionality of hardness to the flow stress), due to fine, coherent and ordered precipitates with radius of r and volume fraction of f, can be expressed by Eq. (5) [24,29], which has been written for relative percentage of hardening (H_t):

$$\Delta\tau \propto H_t \propto f^{1/2} r^{1/2} \tag{5}$$

Assuming spherical precipitates (for simplification) and site saturation for the nucleation process, the volume fraction of precipitate phase could be simply related to the precipitate radius, as follows [24]:

$$f \propto (4\pi/3) r^3 \Rightarrow r^{1/2} \propto f^{1/6} \Rightarrow H_t \propto f^{2/3} \tag{6}$$

The volume fraction of precipitates (f) could be directly proportional to the volume fraction transformed (X) [24]. Therefore, the volume fraction transformed is related to the relative percentage of hardening as follows:

$$f \propto H_t^{3/2} \Rightarrow X \propto H_t^{3/2} \tag{7}$$

To utilize the modified Avrami equation in the form of $X = 1 - \exp(-(kt)^n)$ [30–33], H_t should be used in normalized form by dividing it to the peak or maximum value of relative percentage of hardening at same temperature (H_m). Therefore:

$$(H_t/H_m)^{3/2} \propto 1 - \exp(-(kt)^n) \tag{8}$$

After some algebra, the following relationship could be derived:

$$\log \ln (H_m^{3/2}/(H_m^{3/2} - H_t^{3/2})) \propto n \log k + n \log t \tag{9}$$

3.4. Calculation of time exponents and activation energy

To obtain the Avrami exponents (time exponents), n, for precipitation reaction in 17-4 PH stainless steel in the hardening portion (up to peak), values of $\log \ln (H_m^{3/2}/(H_m^{3/2} - H_t^{3/2}))$ were plotted versus $\log t$ at different temperatures as shown in Fig. 6. The linear regression of these data (lines with slope of n and intercept of $n \log k$) results in the n values of 0.442, 0.460, 0.472 and 0.484 at 400, 450, 482 and 551 °C, respectively. The value of n can be taken as 0.465 on average for precipitation reaction in 17-4 PH stainless steel. This is relatively consistent with typical value of 0.667 for precipitation on dislocations [34].

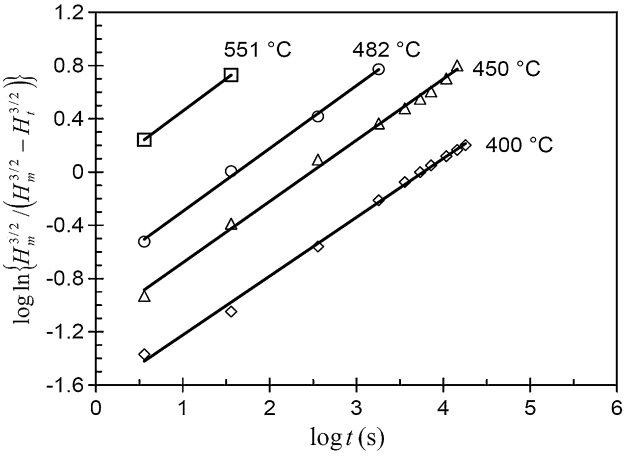

Fig. 6. Plot for calculation of Avrami exponent for precipitation reaction.

The temperature dependence of transformation kinetics has been estimated by the following Arrhenius equation [33]:

$$k = k_0 \exp(-Q/RT) \tag{10}$$

or

$$\ln k = \ln k_0 + (-Q/R)(1/T) \tag{11}$$

To obtain the activation energy, Q, for precipitation reaction (nucleation and growth) in 17-4 PH stainless steel, k values were determined from regression analysis of Fig. 6 and subsequently the values of $\ln k$ were plotted versus $1/T$ (T is in Kelvin) as shown in Fig. 7. The linear regression of these data results in the Q value of 262 kJmol^{-1}. This is consistent with the expected value of 283.9 kJmol^{-1} for diffusion of copper in ferrite [35]. In a previous study, the precipitation activation energy in a 17-4 PH stainless steel has been calculated as 248 kJmol^{-1} using the dilatometric curves [36]. However, in another study [37], the activation energy for precipitation in a 17-4 PH alloy has been calculated as 112.2 kJmol^{-1} from the resistivity measurements.

Previous investigations [30–32,38–42] on the precipitation kinetics of maraging steels have shown that Avrami exponents from kinetic equations have values ranging from 0.2 to 0.5. These are well below expected values for various nucleation and growth processes. The apparent activation energies for precipitation in these alloys were in the range of 79–196 kJmole^{-1} [30–32,38–42], considerably lower than typical values for diffusion of corresponding elements (e.g. Ni and Al) in ferrite. The low time exponents and apparent

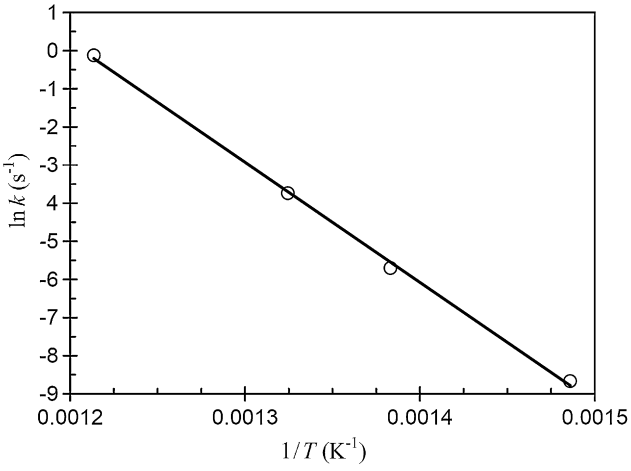

Fig. 7. Plot for calculation of activation energy for precipitation reaction.

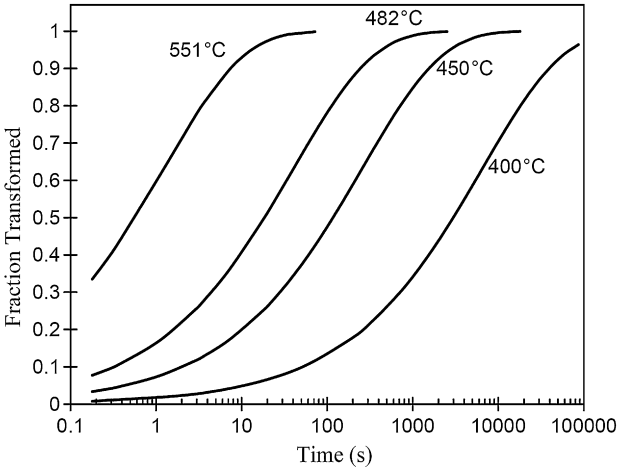

Fig. 8. Precipitation kinetics during isothermal aging for 17-4 PH stainless steel.

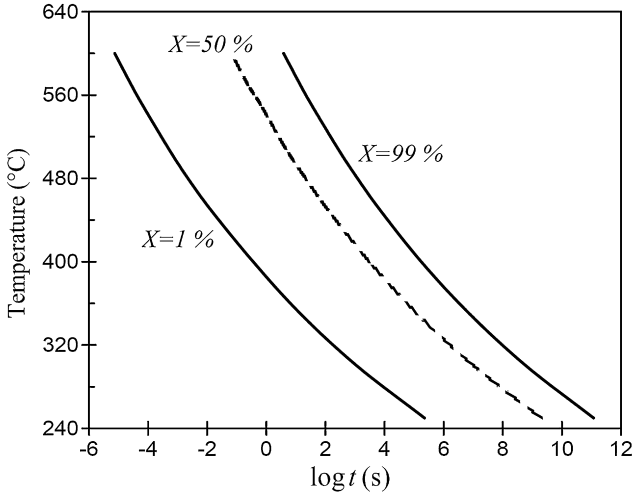

Fig. 9. Time-temperature-transformation diagram for copper precipitation in 17-4 PH stainless steel.

activation energy values have been attributed to the nucleation of intermetallic phases along or near dislocations, followed by growth of the precipitates via enhanced dislocation pipe diffusion. The aforementioned interpretation is reasonable due to high dislocation density associated with the martensitic matrix in these alloys [24].

In the case of the present investigation, the calculated low Avrami exponents can be ascribed to the enhanced nucleation rate of copper due to the high dislocation density in as-quenched lath martensitic structure. In other words, precipitation generally tends to start on dislocations, boundaries of lath martensite or boundaries of prior austenite grains, where the least energy is required for precipitation process. Furthermore, the calculated activation energy for precipitation is consistent with the expected value of 283.9 kJmol^{-1} for diffusion of copper in ferrite.

3.5. Precipitation progress and its rate

Based on Avrami analyses, the following formula could be derived for precipitation reaction in 17-4 PH stainless steel at the hardening stage:

$$X=1-\exp\left\{-\left(e^{38}\times\exp\left(-\frac{261.87\times10^3}{8.314\times T}\right)\right)^{0.465}\times t^{0.465}\right\} \quad (12)$$

or

$$X=1-\exp\left\{-e^{17.67}\times\exp\left(-\frac{121.77\times10^3}{8.314\times T}\right)\times t^{0.465}\right\} \quad (13)$$

where T is temperature in Kelvin and t is time in second.

Fig. 8 shows the volume fraction transformed, X, as a function of time at various temperatures. The curves exhibit typical sigmoidal form (S-shaped). However, no classical (sharp) incubation period is detected in these precipitation curves. The early increase in rate of precipitation is followed by a linear region, and finally the rate of precipitation decreases and tends toward zero.

Fig. 9 shows the fraction transformed as a function of temperature and time in the form of time-temperature-transformation (TTT) diagram. It is apparent from this figure that the precipitation rate increases by increasing aging temperature. The incubation period for the onset of precipitation at conventional aging temperatures (above 482 °C, see Table 1) is very short. Therefore, there is no significant free energy barrier for the nucleation process at these temperatures [37].

The transformation rate can be estimated by the reciprocal of the time corresponding to precipitation fraction of 0.5 or 50% ($1/t_{0.5}$). Fig. 10 shows the dependence of $1/t_{0.5}$ on aging temperature. Analysis of the curve, results in the following relationship for precipitation rate in 17-4 PH stainless steel:

$$\text{Rate}=\frac{1}{t_{0.5}}\propto\exp(0.0566\times T) \quad (14)$$

Eq. (14) provides useful information about precipitation kinetics. For instance, precipitation rate at 482 °C is about 100 and 1750 times greater than precipitation rate at 400 and 350 °C, respectively. This is apparent that aging temperature has a great impact on the rate of precipitation, and the precipitation kinetics at low temperatures is very slow.

3.6. Controversies on activation energy calculation

Avrami equation in the form of $X=1-\exp(-kt^n)$ accompanying with temperature dependence of transformation kinetics in the form of $k=k_0\exp(-Q/RT)$ yields to the Q value of 115.6 kJmol^{-1}. This is close to a previously reported value for this steel (112.2 kJmol^{-1}) [37]. However, based on the Avrami equation of $X=1-\exp(-(kt)^n)$ accompanying with $k=k_0\exp(-Q/RT)$, the value of 262 kJmol^{-1} was obtained for Q. The question remains to be answered: Which kinetic equation should be used for calculation

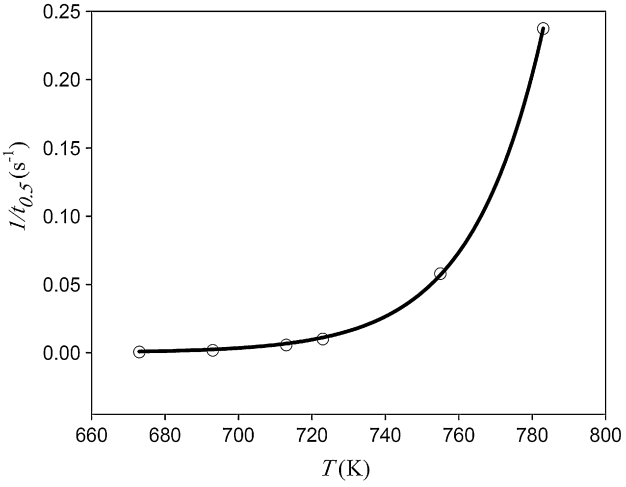

Fig. 10. Precipitation rate as a function of aging temperature for 17-4 PH stainless steel.

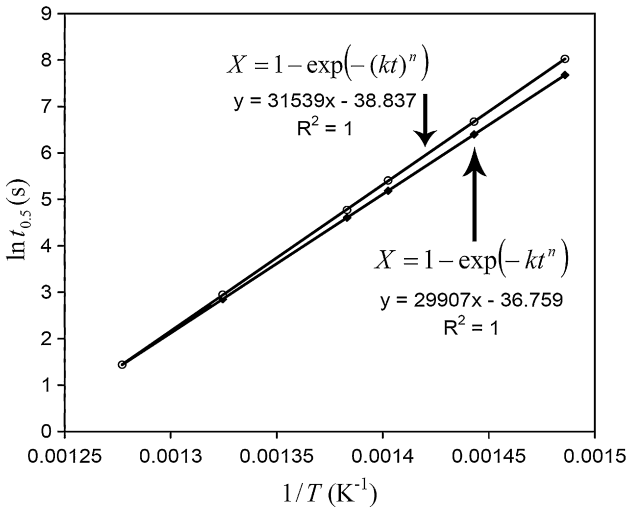

Fig. 11. Calculation of activation energy using the time for constant fraction technique.

of activation energy? In order to solve this problem, an alternative method was used for calculation of activation energy.

It is widely accepted that the overall rate of the transformation process in its general form may be expressed by [43]:

$$\frac{dX}{dt} = [f(X)]k_0 \exp\left(-\frac{Q}{RT}\right) \quad (15)$$

where $f(X)$ is a function of X only. Integration of this equation from 0 to $t_{0.5}$ results in:

$$\int_0^{t_{0.5}} dt = \exp\left(\frac{Q}{RT}\right) \times \int_0^{0.5} [k_0 f(X)]^{-1} dX \quad (16)$$

After some algebra, the following relationship could be derived:

$$\ln t_{0.5} = \left(\frac{Q}{R}\right)\left[\frac{1}{T}\right] + \ln\left\{\int_0^{0.5} [k_0 f(X)]^{-1} dX\right\} \quad (17)$$

It follows from this expression that the slope of the plot of $\ln t_{0.5}$ against reciprocal of absolute temperature can be used for obtaining the value of Q/R. This method is known as "the time for constant fraction technique" [43]. The plots of $\ln t_{0.5}$ vs. $1/T$ (T is in Kelvin) for both forms of kinetics equations are shown in Fig. 11. The activation energies from kinetics equations of $X = 1 - \exp(-kt^n)$ and $X = 1 - \exp(-(kt)^n)$ are calculated as 248.6 (consistent with [36]) and 262.2 kJmol^{-1} (consistent with Section 3.4), respectively. The two kinetics equations yield relatively similar results which are consistent with the activation energy for diffusion of copper in ferrite. It can be concluded that choosing the inappropriate combination of kinetics equations may significantly alter the calculated activation energy and may yield completely different interpretation of results.

4. Conclusions

(1) The effect of aging temperature and time on the hardening behavior of 17-4 PH stainless steel was modeled and analyzed by means of artificial neural networks (ANNs).
(2) At low tempering parameters, the increase in hardness is very low. At higher values up to peak point, the hardness increases due to precipitation of Cu. A softening process, probably recovery of martensite, becomes more effective after an inflection point in this range. After peak point, the hardness decreases due to precipitate coarsening, recovery, and also the reversion of martensite to austenite.
(3) The hardness increases gradually with time at lower temperatures and rapidly at higher temperatures to a peak value. Moreover, the hardness decrease beyond peak point is more prominent at higher temperatures.
(4) Using Avrami analyses for precipitation kinetics of 17-4 PH stainless steel, the average value of time exponent (n) was found as 0.465. This low value can be ascribed to the enhanced nucleation rate of copper in the highly dislocated martensitic matrix.
(5) Precipitation rate showed an exponential dependence on aging temperature: Rate $\propto \exp(0.0566 \times T)$.
(6) Activation energy for precipitation reaction was determined as 262 kJmol^{-1} which is consistent with the expected value of diffusion of copper in ferrite (283.9 kJmol^{-1}). It has been shown that for correct calculation of activation energy, the combination of $X = 1 - \exp(-(kt)^n)$ and $k = k_0 \exp(-Q/RT)$ or the time for constant fraction technique could be used.

References

[1] R.A. Lula, Stainless Steel, ASM, Metals Park, OH, 1986, p. 80.
[2] J.C. Lippold, D.J. Kotecki, Welding Metallurgy and Weldability of Stainless Steels, Wiley Interscience, Hoboken, NJ, 2005, p. 264.
[3] C.N. Hsiao, C.S. Chiou, J.R. Yang, Mater. Chem. Phys. 74 (2004) 134.
[4] H.J. Rack, D. Kalish, Metall. Trans. A 5 (1974) 1595.
[5] U.K. Viswanathan, S. Banerjee, R. Krishnan, Mater. Sci. Eng. A 104 (1988) 181.
[6] AK Steel, 17-4 PH-B-08-01-07, http://www.aksteel.com, 2007.
[7] M. Murayama, Y. Katayama, K. Hono, Metall. Mater. Trans. A 30 (1999) 345.
[8] J. Wang, H. Zou, C. Li, S. Qiu, B. Shen, Mater. Charact. 57 (2006) 274.
[9] J.H. Wu, C.K. Lin, J. Mater. Sci. 38 (2003) 965.
[10] J. Wang, H. Zou, C. Li, R. Zuo, S. Qiu, B. Shen, J. Univ. Sci. Technol. Beijing 13 (2006) 235.
[11] P. Li, Q.Z. Cai, B.K. Wei, X.Z. Zhang, J. Iron Steel Res. Int. 13 (2006) 73.
[12] Metal Ravne, Steel PK346, http://www.metalravne.com, 2005.
[13] S. Isogawa, H. Yoshida, Y. Hosoi, Y. Tozawa, J. Mater. Process. Technol. 74 (1998) 298.
[14] J.R. Davis, Alloy Digest Sourcebook: Stainless Steels, ASM International, Materials Park, OH, 2000, p. 369.
[15] J.H. Hollomon, L.D. Jaffe, Trans. Amer. Inst. Min. Metall. Eng. 162 (1945) 223.
[16] H. Kimura, Tetsu Hagane 86 (2000) 343.
[17] K. Hornik, M. Stinchcombe, H. White, Neural Netw. 2 (1989) 359.
[18] H.K.D.H. Bhadeshia, ISIJ Int. 39 (1999) 966.
[19] H. Mirzadeh, A. Najafizadeh, Mater. Des. 30 (2009) 570.
[20] H. Mirzadeh, A. Najafizadeh, Mater. Charact. 59 (2008) 1650.
[21] H. Mirzadeh, A. Najafizadeh, J. Alloys Compd., doi:10.1016/j.jallcom.2008.08.046, in press.
[22] C.M. Bishop, Neural Networks for Pattern Recognition, Clarendon Press, Oxford, 1995.
[23] O.J. Ilegbusi, M. Iguchi, W. Wahnsiedler, Mathematical Physical Modeling of Materials Processing Operations, Chapman & Hall/CRC, Boca Raton, FL, 2000, p. 205.
[24] C.V. Robino, P.W. Hochanadel, G.R. Edwards, M.J. Cieslak, Metall. Mater. Trans. A 25 (1994) 697.
[25] DV.K. Vasudevan, S.J. Kim, C.M. Wayman, Metall. Trans. A 21 (1990) 2655.
[26] A.N. Bhagat, S.K. Pabi, S. Ranganathan, O.N. Mohanty, ISIJ Int. 44 (2004) 115.
[27] J. Lei, P. Liu, X. Jing, D. Zhao, J. Huang, J. Mater. Sci. Technol. 20 (2004) 727.
[28] T. Kinoshita, Y. Tokunaga, H. Endo, J. Jpn Inst. Metals 34 (1970) 233.
[29] D.H. Ping, M. Ohnuma, Y. Hirakawa, Y. Kadoya, K. Hono, Mater. Sci. Eng. A 394 (2005) 285.
[30] D.R. Squires, E.A. Wilson, Metall. Trans. A 15 (1984) 1947.
[31] E.A. Wilson, Scripta Mater. 36 (1997) 1179.
[32] E.A. Wilson, Mater. Sci. Technol. 14 (1998) 277.
[33] H. Nakagawa, T. Miyazaki, J. Mater. Sci. 35 (2000) 2245.
[34] J.W. Christian, The Theory of Transformations in Metals and Alloys, Part 1, Third ed., Pergamon Press, Oxford, 2002, p. 546.
[35] E.A. Brandes, G.B. Brook, Smithells Metal Reference Book, Seventh ed., Butterworth-Heinemann, Oxford, 1992, Chapter 13, p. 19.
[36] R. Kapoor, L. Kumar, I.S. Batra, Mater. Sci. Eng. A 352 (2003) 318.
[37] U.K. Viswanathan, P.K.K. Nayar, R. Krishnan, Mater. Sci. Technol. 5 (1989) 346.
[38] S. Floreen, Metall. Rev. 13 (1968) 115.
[39] D.T. Peters, C.R. Cupp, Trans. Amer. Inst. Min. Metall. Eng. 236 (1966) 1420.
[40] U.K. Viswanathan, T.R.G. Kutty, C. Ganguly, Metall. Mater. Trans. A 24 (1993) 2653.
[41] L.T. Shiang, C.M. Wayman, Mater. Charact. 39 (1997) 529.
[42] D.R. Squires, E.A. Wilson, Metall. Trans. 3 (1972) 575.
[43] A.K. Jena, M.C. Chaturvedi, Phase Transformation in Materials, Prentice Hall, Englewood Cliffs, NJ, 1992, p. 111.